Aerosol and Air Quality Research

Effect of Double Masking with Silk or Cotton Over-masks on the Source Control Capabilities of a Surgical Mask

Adam F. Parlin[1], Mikhail Yermakov[2], Samuel M. Stratton[1,3], Susan R. Reutman[2], Theresa M. Culley[1], Patrick A. Guerra[1*], Sergey A. Grinshpun[2*]

[1] Department of Biological Sciences, University of Cincinnati, Cincinnati, Ohio, USA
[2] Department of Environmental and Public Health Sciences, Center for Health-Related Aerosol Studies, University of Cincinnati College of Medicine, Cincinnati, Ohio, USA
[3] Department of Ecology and Evolutionary Biology, University of Michigan, Ann Arbor, Michigan, USA

ABSTRACT

In spite of the remarkable progress made in the development of safe and effective vaccines against COVID-19, deployment of respiratory protective devices remains vital for mitigating the transmission of SARS-CoV-2 during the ongoing pandemic. In this study, we evaluated double masking, which entails layering a fitted over-mask on top of a surgical mask. A previously validated manikin-based protocol was used to evaluate the performance of a surgical mask with an over-mask made of silk or cotton. We showed that double masking can significantly enhance the mask's source control capabilities by reducing an aerosol emission from a coughing or sneezing wearer while maintaining a reasonable breathability and comfort level. The data obtained in this study, as well as the results recently reported by other investigators, suggest that an over-mask made of silk fabric has several advantages over one made of cotton. Moreover, silk over-masks have the added benefit of providing a reusable protective outer layer for surgical masks as silk is hydrophobic and increases aerosol particle collection. Not only can double masking reduce viral or bacterial transmission, but it can also promote surgical mask longevity, thereby reducing global waste and pollution associated with the use of disposable surgical masks. Finally, an additional study with five human subjects revealed no significant differences in perceived comfort (measured by proxies such as relative humidity, temperature, and CO_2 level inside the mask) between single masking and double masking, as well as between double masking with either a silk or cotton over-mask.

Keywords: Facemask, Source control, Double masking, Silk, COVID-19

1 INTRODUCTION

Considering the significance of airborne transmission of SARS-CoV-2 (Morawska and Milton, 2020), the use of facemasks remains a key public health strategy for mitigating the spread of the virus that underlies the ongoing COVID-19 pandemic. As part of this strategy, surgical masks have been recognized as an important non-pharmaceutical intervention that can help mitigate viral transmission (Chu *et al.*, 2020; Brooks *et al.*, 2021; Gandhi and Marr, 2021). The primary function of face coverings, including surgical masks, is as source control that aims at decreasing the transmission of respiratory secretions (virus-containing larger droplets and smaller aerosol particles) from the wearer to others (Lindsley *et al.*, 2021a, 2021b). Unfortunately, the world has suffered shortages of medical-grade masks and facepiece filtering respirators that necessitated the reuse of disposable protective devices by both healthcare personnel and the general public. These practices required a decontamination/disinfection of these devices, which has often been
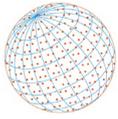
done by utilizing procedures that can negatively impact their integrity and effectiveness (Grinshpun and Yermakov, 2021). Reuse of disposable devices can also lead to a poor fit causing a significant faceseal leakage. Finally, the commercially available disposable particle filtering facepieces are typically composed of non-biodegradable and non-renewable materials so that their disposal during pandemic represents a significant environmental challenge harming various ecosystems (Rathinamoorthy and Balasaraswathi, 2021; Selvaranjan et al., 2021).

To address the limitations of surgical masks and improve their utility as a source control method, double masking, also known as over-masking, has been explored. For example, a less efficient face covering such as a cloth-based mask can be worn on top of a medical-grade mask (Brooks et al., 2021). Double masking can potentially preserve the protective properties of a surgical mask and prolong their useable life by reducing the level of contamination on the mask outer surface (e.g., Parlin et al., 2020). Some models of surgical masks have a layer that is considered hydrophobic; however, only a fraction of commercially available devices possesses this feature. This makes many surgical masks, particularly those that might be used by the general public, vulnerable to becoming wet and contaminated by droplets, which reduces their filtration capacities and longevity. Therefore, double masking with a cloth-based mask, such as one made from silk fabric which is pronouncedly hydrophobic (Parlin et al., 2020), addresses this limitation. We hypothesize that over-masking can also enhance the mask's source control capabilities, which is particularly critical in environments with low availability of vaccines or a substantial hesitancy of the population to vaccination, as well as when mitigating the spread of variants featuring particularly high transmissibility and breakthrough infection rates.

The potential of double masking for maximizing the respiratory protection has been recently investigated (e.g., Arumuru et al., 2021; Sankhyan et al., 2021; Sickbert-Bennett et al., 2021). While studies have examined the effect of double masking on aerosol filtration efficiency, not all of them have tackled a potential decrease in breathability associated with an additional layer or with other factors influencing the comfort level for a wearer. Moreover, in the quoted efforts, the examination of double masking was limited to only one material type used for making fitted over-masks, e.g., a cotton over-mask composed of a single sample of cotton fabric. Meanwhile, the material properties of the fabric utilized for producing a fitted over-mask can be instrumental in making one fabric type more advantageous than another. This includes but is not limited to hydrophobicity which can prevent the underlying surgical mask from getting wet and thus help protect its initial properties (Parlin et al., 2020). Moreover, even a single class of fabric (e.g., cotton) may have significant variation between available samples in key metrics such as weave, porosity, and thickness, which translates to their different impact on performance.

In this study, we examined how double masking can improve the source control properties of surgical masks when a cloth-based face covering is worn as on top of it. Here we focused on the question of how fitted over-masks made of silk or cotton fabrics can enhance the source control capabilities of surgical masks. Silk is advantageous for making face coverings, as we have previously shown this material to be hydrophobic, breathable, light, and reusable after cleaning (Parlin et al., 2020). Silk fabric has naturally inherent, antibacterial and antiviral properties that other fabrics, such as cotton and polyester, do not possess unless these materials are specially treated to acquire them. Several investigators provided scientific evidence of antimicrobial properties of silk (Dong et al., 2013, 2016; Singh et al., 2014; Zhang, 2002; Zhang et al., 2020; Zhu et al., 2020). Silk is composed of fibroin, sericin, and other proteins containing various components with pronounced antimicrobial properties. Hence, we anticipate that different types of silk fabric (from raw to various processed forms) can be utilized for making over-masks and face coverings. In fact, sericin extracted from silk fiber has been used to coat other materials to enhance their antimicrobial and other valuable properties (e.g., Zhang, 2002). A conventional cotton material served as an internal control for the double masking technique examined in this study. Cotton is widely used for face coverings; furthermore, it has been recently utilized for evaluating the double masking concept (Arumuru et al., 2021; Sickbert-Bennett et al., 2021; Sankhyan et al., 2021).

We first tested different silk fabric materials of different thickness and determined their hydrophobicity, particle filter collection efficiency, and breathability (quantified through the pressure drop) in order to down-select the candidates and ultimately identify the best one for making over-masks. Subsequently, we constructed the silk and cotton over-masks' prototypes and tested their ability to enhance the source control properties of a surgical mask using the study protocol
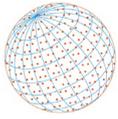
described in Grinshpun and Yermakov (2021). We investigated the transmission of particles aerosolized by the coughing and sneezing manikins wearing a double mask (a conventional surgical mask with either a silk or cotton over-mask) and compared the findings to those obtained with the surgical mask alone. The breathability of the assembled silk- and cotton-based double-mask prototypes was assessed at breathing flow rates representing moderate and strenuous activity levels. In addition to the above-described laboratory study, we performed an evaluation of the silk and cotton over-masks, as well as a surgical mask with no over-masking (control) on 5 human subjects. This phase of the effort allowed us to evaluate the perceived comfort proxies offered by the silk- or cotton-based double masking, which included relative humidity, temperature, and CO_2 concentration at different levels of subjects' physical activity, all measured inside the mask.

2 METHODS

2.1 Silk Materials Chosen for the Study. Quantification of Hydrophobicity. Down-selection

Silk fabric materials representing twenty-one different fabric types were collected from a variety of sources. These materials are listed in Supplementary Table S1 along with their characteristics. For each silk fabric, we measured its thickness (mm) and reported its momme value (if known). Momme is defined as the weight in pounds of a piece of fabric sized 45 inches × 100 yards; one momme (mme) equates approximately 4.34 g m^{-2}. The higher the momme, the heavier and denser the weave is. We used contact angle (CA) to quantify the hydrophobicity of each fabric, assayed by measuring different CA metrics of a 5 µL droplet of water deposited onto the surface of each fabric. For each trial, we measured the starting CA (time = 0), the final CA (time = 2 minutes), and the magnitude change in CA of the water droplet. We measured the dynamic CA of droplets as a measure of the rate of change of the CA from the start to the end of our trials. We also measured the dynamic width and height of the droplet during the trial, to assess how material absorbed the droplet [change in width measures droplet spreading and change in height measures droplet absorption via penetration (Parlin et al., 2020)]. Dynamic CA measurements were taken at 5-second intervals over the 2-minute trial period. Thickness and CA measurements were conducted as described in Parlin et al. (2020), and each silk material was tested with 3 replicates.

Following the hydrophobicity testing (see above) and applying additional criteria for the tested silk fabrics (e.g., wearability, weight, density, and porosity), we narrowed the list of silk fabrics for further testing down to five types (Table 1). These selected fabrics had different thickness and momme values, which allowed us to determine how these characteristics affect the outcome (hydrophobicity level). The five silk materials were subsequently subjected to the particle collection efficiency and pressure drop examinations as described below.

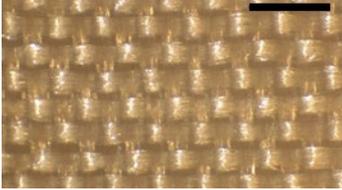### 2.2 Particle Collection Efficiency and Pressure Drop for the Five Selected Silk Single-layer Fabrics
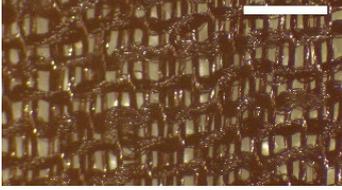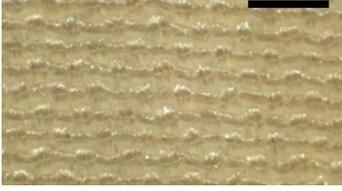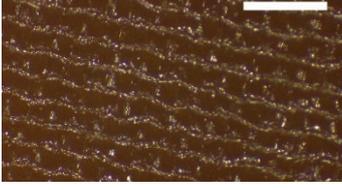
The particle collection efficiency and pressure drop were obtained for these five silk materials (each in a single layer), at two air flow rates: 30 L min^{-1} (moderate workload) and 85 L min^{-1} (strenuous workload). Following a previously used protocol (Reutman et al., 2021), the concentrations of aerosolized particles were measured upstream and downstream of the tested material size selectively in a range of 0.04–8.10 µm using an Electric Low-Pressure Impactor (ELPI, Dekati Ltd., Kangasala, Finland), and the size-specific collection efficiencies were determined based on these aerosol concentration measurement results. The pressure drop for a single layer was measured in triplicate using a Digital Differential Pressure Gauge (Model DM-1103, Dwyer Instruments Inc., Michigan City, IN, USA).

2.3 Final Down-selection of the Silk Fabric and Double-mask Prototyping

Based on the results obtained by examining the hydrophobicity, collection efficiency, and breathability of the five single-layer silk materials (Table 1), we selected the best one that was implemented in the over-mask prototype. The cotton material (used as control) was cut off a 100% cotton, 400 thread count pillow case. The silk and cotton over-masks adopted the design
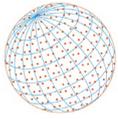
Table 1. Images and characteristics including material thickness, known momme value, and starting and final contact angle (CA) of the five silk fabrics selected for specific testing in this study. For material thickness and CA measurements, values represent the mean $\pm$ standard error of the mean for the three replicate measurements. Lines in images are scale bars equivalent to 1 mm. Asterisk indicates silk materials from Parlin et al. (2020).

Image	Material ID	Thickness (mm)	Momme	Starting CA	Final CA
	Wyoming White Silk Scarf	0.072 $\pm$ 0.001	8	40.18 $\pm$ 3.23	0 $\pm$ 0
	Black Silk Scarf*	0.094 $\pm$ 0.002	8	123.97 $\pm$ 0.68	97.02 $\pm$ 26.50
	White Silk Pillowcase	0.147 $\pm$ 0.002	19	121.03 $\pm$ 7.12	71.83 $\pm$ 2.94
	Black Mulberry Pillowcase*	0.165 $\pm$ 0.001	21	116.05 $\pm$ 2.49	14.04 $\pm$ 1.32
	White Silk Pillowcase	0.212 $\pm$ 0.005	30	121.83 $\pm$ 2.03	87.69 $\pm$ 2.87

of a commercially available and commonly used surgical mask (Model 1818, 3M Corp., St. Paul, MN, USA). Each over-mask was made from a single piece of 9" × 17" silk or cotton material, similar to the protocol used in Reutman et al. (2021) (see Supplementary Materials for details on the construction of over-masks). Each 9" edge was inverted and sewed shut to create a 1/8" closed seam. The material was then folded in thirds lengthwise, with approximately 6" on the right side folded towards the center, and 3" of the left side folded over to overlap the opposite side. The short edges were then sewn together, and the entire piece was turned inside out. Three sets of pleats, approximately equally spaced, were created lengthwise across the mask by pinching the material and fixing the pleats in place by sewing along the edges. Ties made from 45" flat sport shoelaces (PEAK Brand, Providence Products, Charlotte, NC, USA) were then centered along the side edges of each mask and sewn in place, so that they could be used to tie the mask over the user's head and from behind. The over-mask's dimensions permitted it to completely cover the under-mask. The over-mask – either silk or cotton – was positioned to fit over the 3M Model 1818 surgical mask and affixed with ties overhead and from behind. The double mask prototype was designed to eliminate gaps near the nose area and at the sides, which are common areas of air leakage.

2.4 Pressure Drop for the Double-mask Prototype
The breathability of double masks with either a silk or cotton over-mask was examined through
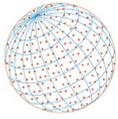
the pressure drop measurements at air flow rates of 30 and 85 L min^{-1}. This examination was conducted with the prototypes donned on the manikin headform.

2.5 Concentration Patterns of Aerosol Emitted by a Coughing and Sneezing Manikin under Different Masking Conditions

Using the experimental set-up and protocol outlined in Grinshpun and Yermakov (2021), we tested the aerosol emission from a coughing and sneezing human manikin under three different masking conditions. This phase of the study was performed to evaluate how over-masks (silk or cotton) enhance the source control properties of surgical masks.

The manikin headform of 22 cm high with an oval cross-section of 20 cm (ear-to-ear) by 24 cm (depth) and a distance from the back of the head to the lips of 22 cm, connected to either a coughing or sneezing simulator, was positioned in the center of a 24-m^3 aerosol test chamber. The aerosol particles were generated from a 50% water-based protein solution and expelled forward from the emission point between the lips. The total aerosol concentration was measured in real time using a condensation particle counter (CPC, P-Trak, TSI Inc., Shoreview, MN, USA) within the sub-micrometer (< 1 μm) particle size range covering a single aerosolized SARS-CoV-2 virus (≈ 0.1 μm) as well as virus agglomerates and virus-carrying particles. It is worth noting that the size ranges of particles generated by coughing and sneezing, which have been reported in several studies, varied substantially. The particle sizes measured are dependent on the sampling point (specifically, the distance from the source), relative humidity, type of the aerosol instrument used, and other factors. The evaporation rate of larger droplets released by expiratory activities is the key parameter determining the particle size range reported in the literature. For example, the study by Yang et al. (2007) refers to 82% of droplets, by number, being in the range of 0.74–2.12 μm, which includes super-micrometer particles (> 1 μm). At the same time, the other investigation, Zayas et al. (2012), published 5 years later, stated that sub-micrometer particles (< 1 μm) "represented 97% of the total number of measured droplets contained in the cough aerosol." Based on the review of multiple studies on indoor aerosol particles released by expiratory activities, we concluded that the sub-micrometer size range offered by the P-Trak instrument is suitable for characterizing the aerosol emission from a coughing and sneezing manikin in the indoor space around this manikin.

The measurements were carried out in the nodes of a horizontally oriented 2D polar coordinate system with the aerosol emission point designated as zero. Each point on the plane was determined by the distance from the emission point (30, 60, and 90 cm) and the angle from the front-forward direction (0°, 30°, 60°, 90°, 120°, 150°, 180°, 210°, 240°, 270°, 300°, and 330°). Altogether, the aerosol concentration was obtained at 36 points with each value calculated as an average of 10 CPC readings. Each concentration measurement was conducted in three replicates, and the arithmetic average was calculated and recorded accordingly. The tests were performed with the 3M Model 1818 surgical mask alone, the same surgical mask with the silk over-mask, and the same surgical mask with the cotton over-mask. The two-dimensional spatial patterns were established for specific concentrations of coughing- and sneezing-generated aerosols. The concentration isolines were drawn to visualize the patterns. Each isoline corresponds to a specific aerosol concentration value calculated as the background level multiplied by 5, 10, or 20. The latter is referred to as Excess Factor relative to the background (Grinshpun and Yermakov, 2021). This approach allows assessing the exposure to the CPC-measured submicrometer aerosol particles in the vicinity of a mask-wearing "spreader."

2.6 Perceived Comfort Proxies

The next phase was a pilot study aimed at assessing the perceived comfort proxies for the surgical mask as well as the silk- or cotton-based double mask prototypes. These included the relative humidity, temperature, and the CO_2 concentration measured inside the masks with a Traceable High Range Datalogging CO_2 Meter (Model CNC-6526, Mitchell Instrument Co., Vista, CA, USA). Five human subjects were recruited, medically cleared and tested at two different levels of physical activity (low and moderate) while wearing the three above-listed protective devices. Sitting represented a low activity level and walking represented a moderate one. The human subject study protocol and consent form were approved by the University of Cincinnati Institutional Review Board.
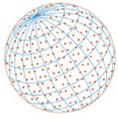
2.7 Data Analysis

To assess the hydrophobicity of different silk fabrics, the CA data were analyzed. This included both the starting and final CA, and the magnitude change in CA over 2 minutes. A one-way ANCOVA was deployed for each of these metrics, with material thickness as a covariate. Dynamic CA, droplet height, and droplet width for the different silk materials were analyzed using a linear mixed-effect model with the silk material as the fixed effect, the trial number as a random effect to account for repeated measures, and an autocorrelation structure to account for temporal autocorrelation within each trial. We compared each separate model against a null using a likelihood ratio test and reported the conditional and marginal r^2 (Sotirchos et al., 2019) for each analysis. An estimated marginal means squared posthoc comparison was used for pairwise comparisons (Russell, 2018). All CA data were analyzed in R (R core Team, 2019). Significance was set to $\alpha = 0.05$ except when adjusted for multiple pairwise comparisons. In our analyses, we report statistical significance (p-values) and effect sizes (η_p^2: starting CA, final CA, magnitude change in CA analyses; marginal and conditional r^2 for dynamic CA analyses).

We examined and compared the particle collection efficiency and pressure drop measurements for the five chosen silk fabrics, to determine how these parameters were affected by the properties of silk fabric (e.g., the thickness and momme). For particle collection efficiency, we used a one-way ANOVA to compare the efficiency curves over the size range of 0.04–8.10 μm determined at two air flow rates (Reutman et al., 2021). We also used a one-way ANOVA to compare the mean pressure drop measurements (mean of three replicate measurements) of the five silk fabrics at the two tested air flow rates.

Similar to our earlier study (Grinshpun and Yermakov, 2021), the particle concentration patterns were visually compared in the vicinity of the coughing or sneezing manikin for the double masking scenario with either a silk or cotton over-mask versus the conventional scenario involving the surgical mask alone. The pressure drop values obtained at two tested air flow rates were compared using a two-way ANOVA.

Finally, we compared surgical mask alone, with both double masking conditions (either a silk or cotton over-mask), in terms of three proxies of comfort (relative humidity, temperature, and the CO_2 concentration). This comparison was performed using separate two-way repeated measures ANOVAs. The mean of three replicate measurements for each of the five human subjects were recorded as data points, in each of the different treatment combinations involving our two treatment factors (Factor 1 – activity level: low or moderate; Factor 2 – double masking treatment: surgical mask alone, surgical mask and cotton over-mask, or surgical mask and silk over-mask). All of these analyses were conducted in the R-based statistical program Jamovi (2021). Here, we report the statistical significance of tests (p-values) with significance set to $\alpha = 0.05$, as well as estimates of effect sizes (η^2).

3 RESULTS

3.1 Hydrophobic Properties of Silk Materials

The hydrophobicity of the 21 initially tested silk fabrics listed in Supplementary Table S1 varied substantially. For example, the range of starting CAs extended from $123.97 \pm 0.68°$ (strong hydrophobicity) to $40.18 \pm 3.23°$ (weak hydrophobicity) and final CAs from $117.40 \pm 1.60°$ (strong hydrophobicity) to $0°$ (water droplet completely absorbed by the material at the end of the trial). When comparing the starting CA (ANCOVA: $F_{20,21} = 25.62$, $p < 0.001$, $\eta_p^2 = 0.96$), final CA (ANCOVA: $F_{20,21} = 185.36$, $p < 0.001$, $\eta_p^2 = 0.99$), and the magnitude of change in CA (ANCOVA: $F_{20,21} = 57.09$, $p < 0.001$, $\eta_p^2 = 0.98$), we found that the materials differed from one another in terms of hydrophobicity. The thickness of the silk fabrics influenced neither their level of hydrophobicity as measured by starting CA (ANCOVA: $F_{1,21} = 1.32$, $p = 0.26$, $\eta_p^2 = 0.06$) and final CA (ANCOVA: $F_{1,21} = 0.069$, $p = 0.80$, $\eta_p^2 = 0.003$), nor the magnitude change in CA during the trial (ANCOVA: $F_{1,21} = 0.48$, $p = 0.49$, $\eta_p^2 = 0.02$). There was no interaction between the type of examined fabric and its thickness for starting CA measurements (ANCOVA: $F_{20,21} = 1.45$, $p = 0.20$, $\eta_p^2 = 0.58$), but there were significant interactions between fabric type and thickness for final CA (ANCOVA: $F_{20,21} = 4.68$, $p < 0.001$, $\eta_p^2 = 0.81$) and magnitude change in CA (ANCOVA: $F_{20,21} = 1.63$, $p < 0.01$, $\eta_p^2 = 0.74$). These results indicate that the maintenance or change in hydrophobicity of silk over time can
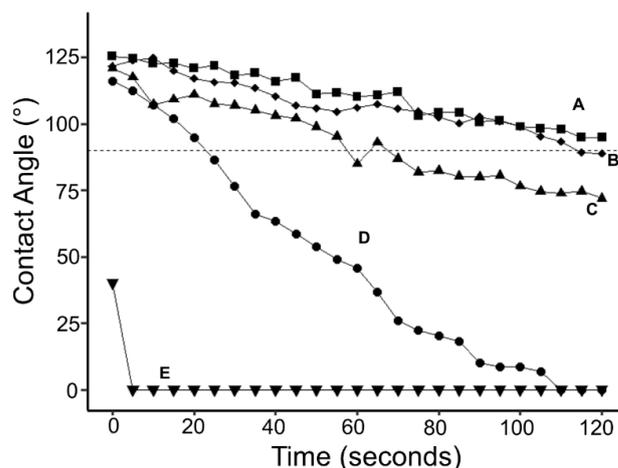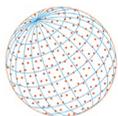
Fig. 1. Dynamic contact angle for five down-selected silk fabrics as measured in hydrophobicity trials (Table 1). (A) Black Silk Scarf (0.094 mm, 8 mme; squares), (B) White Silk Pillowcase (0.212 mm, 30 mme; diamonds), (C) White Silk Pillowcase (0.147 mm, 19 mme; upright triangles), (D) Black Mulberry Pillowcase (0.165 mm, 21 mme; circles), and (E) Wyoming White Silk Scarf (0.072 mm, 8 mme; upside down triangles). The dotted line (contact angle = 90°) represents the threshold for hydrophobic (> 90°; incomplete wetting) and hydrophilic (< 90°; increased wetting) materials. Error bars for each individual data point are omitted for clarity.

depend on the type of silk examined and its corresponding thickness. When examining dynamic CA as a measure of hydrophobicity, we found that materials with lower known momme values were less hydrophobic than those with higher momme value, as indicated by the significant difference in the dynamic CA as a function of material type (χ^2 = 367.66, df = 20, p < 0.001; marginal r^2 = 0.83, conditional r^2 = 0.83).

Therefore, from this variety of materials, the following five (Table 1) were selected that featured different thickness and momme values (listed by thickness from low to high): Wyoming White Silk Scarf (0.072 mm, 8 mme); Black Silk Scarf (0.094 mm, 8 mme); the 19-mme White Silk Pillowcase (0.147 mm, 19 mme); unwashed Black Mulberry Pillowcase (0.165 mm, 21 mme); and the 30-mme White Silk Pillowcase (0.212 mm, 30 mme). Fig. 1 presents the dynamic CA of water droplets as a function of time determined for these five silk materials. The dotted line (CA = 90°) represents the threshold for hydrophobic (> 90°; incomplete wetting) and hydrophilic (< 90°; increased wetting) materials. There was a difference in hydrophobicity between the two silk materials featuring the same momme value (8 mme). The Wyoming White Silk Scarf had rapid spreading and absorption of the water droplet, whereas the Black Silk Scarf maintained the droplet on top of the surface. This difference is attributed to the Black Silk Scarf having a denser and less porous weave pattern to the material (Parlin et al., 2020). The 19 mme and 30 mme fabrics maintained the droplet on top of the surface. Similarly, the 21 mme fabric had strong initial hydrophobicity, but the water droplet was absorbed by the end of the trial. The shift in hydrophobicity observed for the 21 mme silk during the trial is likely caused by its less dense weaving pattern. Overall, these data reveal that hydrophobicity of silk fabrics can vary substantially between different silk types. In general, silk fabrics with higher momme are more hydrophobic than those of lower ones. In some instances, however, lower momme silk can still have high hydrophobicity, for example, if the weaving pattern of the silk is dense. The weave pattern of the silk fabric also affects how hydrophobicity values can change over time (Fig. 1).

3.2 Particle Collection efficiency and Pressure Drop for the Five Selected Silk Single-layer Fabrics

Overall, all of the five selected silk fabrics (Table 1) provided relatively poor particle collection efficiency across the tested size range. The highest single-layer efficiencies were observed at both air flow rates for the Black Silk Scarf, the 19-mme White Silk Pillowcase, and the 30-mme White Silk Pillowcase. However, even these five materials collected less than 50% particles across the
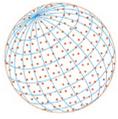
tested size range. The other two materials collected as low as < 25% of particles at both flow rates. For comparison, an N95 respirator filter collects > 95% of aerosol particles of the most penetrating particle size at 85 L min^{-1}. Generally, the particle size-specific and overall collection efficiencies of the tested silk fabric falls within the range reported by Reutman et al. (2021) for household materials used for making homemade facemasks. It is noted that since this study is concerned with the control of aerosol emission from a mask wearer to the environment, rather than protection of a wearer, an improvement of the collection efficiency provided by double masking is not a primary focus of this effort.

An increase of the air flow rate from 30 to 85 L min^{-1} resulted in a significant decrease of collection efficiency, which is explainable considering that the challenge aerosol particles were predominantly in the submicrometer size range containing an appreciable ultrafine fraction.

The pressure drop determined in three replicates for a specific fabric under a given set of conditions showed no measurable data variability because the between-test variability was lower than the limit of detection of the Digital Differential Pressure Gauge (0.05 mm w.g.). Thus, the pressure drop data readings were recorded and analyzed as single values. Consequently, we could not deploy ANOVA, as planned, to statistically analyze the effect of flow rate on the pressure drop, because the variability of the replicate pressure drop measurements was not quantifiable. Based on the comparison of single values, it was concluded that the flow rate effect was substantial: an increase from 30 to 85 L min^{-1} resulted in a several-fold increase in the pressure drop, depending on the silk material tested.

The single-layer pressure drop values varied significantly from one silk material to another, but – under all the test conditions – they did not exceed 4 mm w.g. The pressure drop was generally higher the thicker the silk fabric was. The relatively low pressure drop values determined in this study, ranging from the limit of detection (0.05 mm w.g.) for the Black Silk Scarf at 30 L min^{-1} to 3.5 mm w.g. for the 30 mme White Silk Pillowcase at 85 L min^{-1}, suggest acceptable breathability of a single layer. Furthermore, even a double- or triple-layer configuration is deemed breathable as the pressure drop for the least permeable of the five silk fabrics was approximately 10 mm w.g. Thus, any of the five selected materials appears feasible for the respiratory protection application.

3.3 Pressure Drop for Silk and Cotton Double-mask Prototypes

Following a comprehensive review of the data gathered on hydrophobicity, collection efficiency, and breathability as well as considering additional factors (e.g., wearability, weight, density, and porosity of the selected silk fabric types), we chose the 30-mme White Silk Pillowcase and cotton (double-layered, pleated) for the double-mask prototypes. The prototypes constructed with these materials were subjected to the breathability examination on the manikin. It was found that the pressure drop values were close to each other for a fixed flow rate although silk was slightly more breathable: 2.59 mm w.g. (silk) and 2.81 mm w.g (cotton) at 30 L min^{-1}, and 8.75 mm w.g. (silk) and 9.11 mm w.g. (cotton) at 85 L min^{-1}. Although these values were obviously greater than those obtained for the single-layer materials, the double-mask prototypes still offer comfortable breathability (Kim et al., 2015) and fall well below the NIOSH-permitted filter airflow resistance thresholds for inhalation (35 mm w.g.) and exhalation (25 mm w.g.) (Code of Federal Regulations, 2013).

3.4 Aerosol Concentration Patterns around a Coughing and Sneezing Manikin: Effect of Double-masking on the Source Control Capabilities

Fig. 2 presents the aerosol concentration patterns by depicting the background Excess Factor isolines. It is noted that the cross-section of the manikin headform is slightly off-center to reflect the location of the aerosol emission point.

The elevated exposure zones notably shrunk when moving from the surgical mask alone to the double mask (with either silk or cotton over-masking). The double masking enhances the source-control effectiveness as it significantly impedes the spread of aerosol particles in the vicinity of the manikin. Both silk and cotton over-masks performed similarly. The coughing and sneezing data sets show similar trends with some differences partially attributed to different durations of the aerosol generation cycles between the two simulated activities. The latter finding is consistent with the results reported earlier (Grinshpun and Yermakov, 2021).
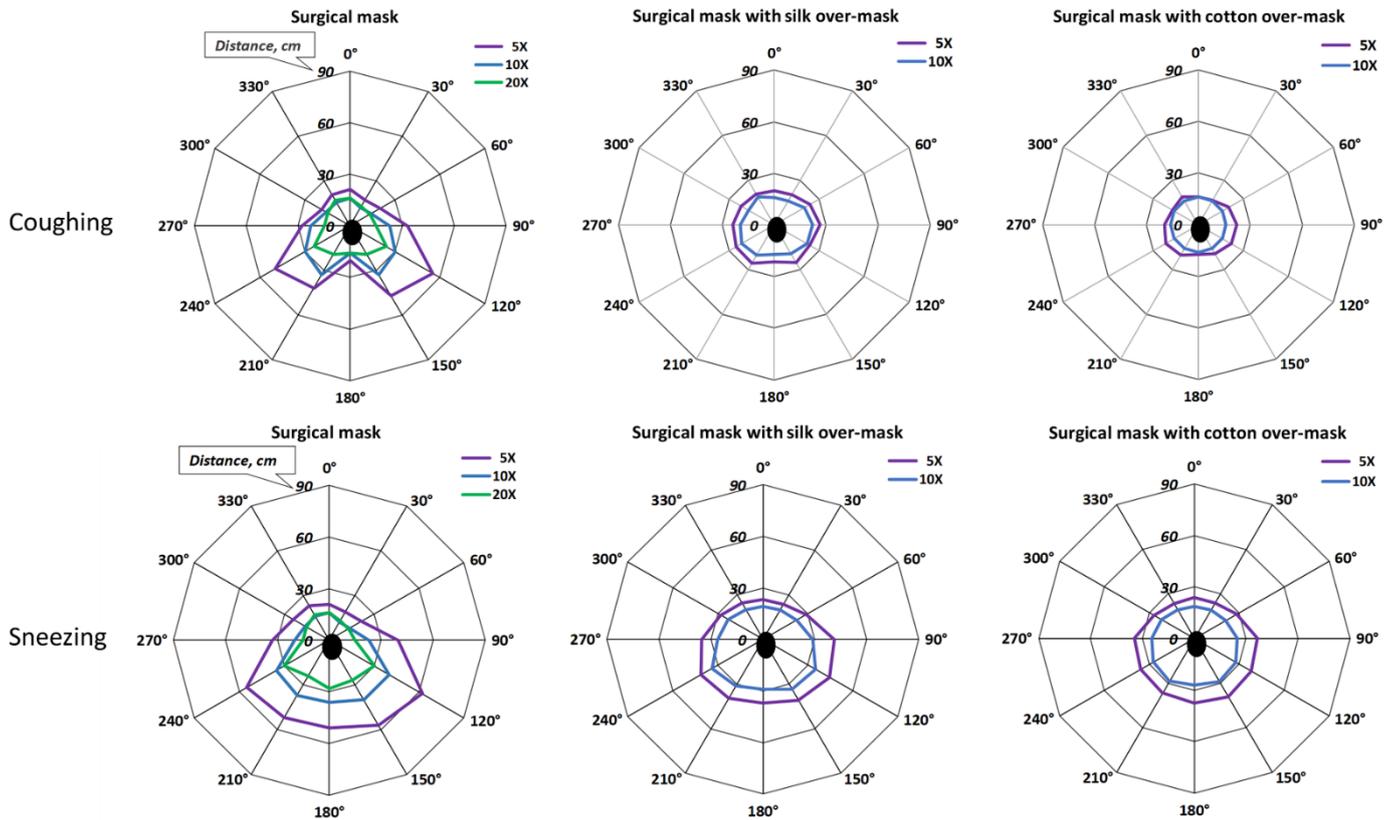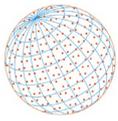
Fig. 2. Isoline patterns for aerosol concentration measured during coughing (top row) and sneezing (bottom row), comparing surgical mask alone with double masking utilizing either a silk or cotton over-mask. Each color represents a specific concentration Excess factor compared to background: 5, 10, and 20.

3.5 Relative Humidity, Temperature, and CO₂ Concentration as Perceived Comfort Proxies

The pilot study involving human subjects and comparing single and double masking with either a silk or cotton over-mask showed that for relative humidity, there was no interaction between activity level and double masking treatment (two-way repeated measures ANOVA, interaction: F = 2.68, df = 2, p = 0.129, η^2 = 0.028). The mean values from the two activity levels (low and moderate) were similar for the three tested scenarios: only a surgical mask was worn, a silk over-mask was layered over the surgical mask, and cotton over-mask was layered over the surgical mask. There was no effect of double masking treatment (main effect: F = 1.39, df = 2, p = 0.304, η^2 = 0.047), with silk and cotton over-masks functioning similarly. There was an effect of activity level (main effect: F = 526.81, df = 1, p < 0.001, η^2 = 0.0540), with the low activity level corresponding to a slightly greater humidity compared to the moderate activity level. Although statistically significant, the difference in the subject activity level generated a very minor effect on relative humidity (~5%). For temperature, there was no interaction between activity level and double masking treatment (two-way repeated measures ANOVA, interaction: F = 1.3538, df = 2, p = 0.312, η^2 = 0.025). There was no effect of activity level (main effect: F = 6.0579, df = 1, p = 0.070, η^2 = 0.110) and no effect of double masking treatment (main effect: F = 0.0188, df = 2, p = 0.981, η^2 = 0.001). Finally, for CO₂ concentration, there was no interaction between activity level and double masking treatment (two-way repeated measures ANOVA, interaction: F = 0.0341, df = 2, p = 0.967, η^2 = 0.001). There was no effect of activity level (main effect: F = 0.8504, df = 1, p = 0.409, η^2 = 0.016) and no effect of double masking treatment (main effect: F = 0.4667, df = 2, p = 0.643, η^2 = 0.048). Overall, we found no differences in perceived comfort (quantified by the three selected proxies of comfort) between single masking and double masking. In addition, we concluded that there were no differences in perceived comfort for double masking with either a silk or cotton over-mask.
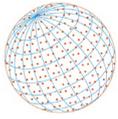
4 CONCLUSIONS

We found support for our hypothesis that over-masking enhances the mask's source control capabilities. The data suggest that double masking can significantly decrease the spread of aerosol particles emitted by a coughing or sneezing person as compared to a surgical mask alone. Both silk and cotton over-masks are similarly effective in providing an additional control of the aerosol transmission associated with coughing and sneezing by a mask-wearing person. At the same time, the breathability offered by a double mask remains acceptable in spite of the added over-mask. The over-masking can also boost the aerosol filtration although the quantitative data suggest that adding an extra material does not make a drastic difference for protecting a wearer. Double masking does not decrease the wearer's comfort compared to the single-mask scenario, as determined by the three proxies of comfort (in-mask measured relative humidity, temperature, and CO_2 level). No significant difference was observed in double masking performance or comfort level for the over-masks made of either silk or cotton.

There are benefits associated with the silk over-mask as compared to the cotton over-mask. One benefit of silk material is it has greater hydrophobicity, a valuable property that allows for protecting the surgical mask underneath from effects associated with moisture in the ambient air. Another benefit of using silk over cotton is that silk fabric has inherent antimicrobial properties which can further protect the surgical mask underneath from microbial contamination. In contrast, untreated cotton does not possess these antiviral and antibacterial properties.

Protecting a surgical mask by utilizing double masking prolongs its useable life, thereby reducing waste and conserving vital surgical mask reserves. It is important should a dramatic global shortage was to occur again like it happened during the initial wave of the COVID-19 pandemic. Although silk utilizes resources for producing it as a fabric at an industrial level, silk is a natural, renewable, biodegradable, and relatively long-lasting product. As such, by using a silk over-mask over a surgical mask, double masking with silk can help alleviate the significant environmental costs of using surgical masks alone. Surgical masks, which are to be disposed of after a single use, are non-biodegradable as they are made of plastic – a non-renewable petroleum-based product that has become a significant source of environmental pollution during the COVID-19 pandemic. Considering the special role of masking as a key element of public health strategy during the ongoing COVID-19 pandemic, this study is of a particular importance as it introduces and validates a simple and effective method for enhancing the source control capabilities of masking.

SUPPLEMENTARY MATERIAL

Supplementary material for this article can be found in the online version at https://doi.org/10.4209/aaqr.220036

REFERENCES

Arumuru, V., Samantaray, S.S., Pasa, J. (2021). Double masking protection vs. comfort – A
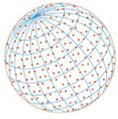
quantitative assessment. Phys. Fluids 33, 077120. https://doi.org/10.1063/5.0058571

Brooks, J.T., Beezhold, D.H., Noti, J.D., Coyle, J.P., Derk, R.C., Blachere, F.M., Lindsley, W.G. (2021). Maximizing fit for cloth and medical procedure masks to improve performance and reduce SARS-CoV-2 transmission and exposure. MMWR Morb. Mortal Wkly. Rep. 70, 254–257. https://doi.org/10.15585/mmwr.mm7007e1

Chu, D.K., Akl, E.A., Duda, S., Solo, K., Yaacoub, S., Schünemann, H.J., Chu, D.K., Akl, E.A., El-harakeh, A., Bognanni, A., Lotfi, T., Loeb, M., Hajizadeh, A., Bak, A., Izcovich, A., Cuello-Garcia, C.A., Chen, C., Harris, D.J., Borowiack, E., Chamseddine, F., *et al.* (2020). Physical distancing, face masks, and eye protection to prevent person-to-person transmission of SARS-CoV-2 and COVID-19: A systematic review and meta-analysis. Lancet 395, 1973–1987. https://doi.org/10.1016/S0140-6736(20)31142-9

Code of Federal Regulations (42 CFR 84.180) (2007). Airflow resistance tests. http://www.gpo.gov/fdsys/pkg/CFR-2007-title42-vol1/pdf/CFR-2007-title42-vol1-sec84-180.pdf (accessed 3 April 2022).

Dong, Z., Zhao, P., Wang, C., Zhang, Y., Chen, J., Wang, X., Lin, Y., Xia, Q. (2013). Comparative proteomics reveal diverse functions and dynamic changes of *Bombyx mori* silk proteins spun from different development stages. J. Proteome Res. 12, 5213–5222. https://doi.org/10.1021/pr4005772

Dong, Z., Song, Q., Zhang, Y., Chen, S., Zhang, X., Zhao, P., Xia, Q. (2016). Structure, evolution, and expression of antimicrobial silk proteins, seroins in Lepidoptera. Insect Biochem. Mol. Biol. 75, 24–31. https://doi.org/10.1016/j.ibmb.2016.05.005

Gandhi, M., Marr, L.C. (2021). Uniting Infectious Disease and Physical Science Principles on the Importance of Face Masks for COVID-19. Med 2, 29–32. https://doi.org/10.1016/j.medj.2020.12.008

Grinshpun, S.A., Yermakov, M. (2021). Technical note: Impact of face covering on aerosol transport patterns during coughing and sneezing. J. Aerosol Sci. 158, 105847. https://doi.org/10.1016/j.jaerosci.2021.105847

Kim, J., Roberge, R.J., Powell, J.B., Shaffer, R.E., Ylitalo, C.M., Sebastian, J.M. (2015). Pressure drop of filtering facepiece respirators: How low should we go? Int. J. Occup. Med. Environ. Health 28, 71–80. https://doi.org/10.13075/ijomeh.1896.00153

Lindsley, W.G., Beezhold, D.H., Coyle, J., Derk, R.C., Blachere, F.M., Boots, T., Reynolds, J.S., McKinney, W.G., Sinsel, E., Noti, J.D. (2021a). Efficacy of universal masking for source control and personal protection from simulated cough and exhaled aerosols in a room. J. Occup. Environ. Hyg. 18, 409–422. https://doi.org/10.1080/15459624.2021.1939879

Lindsley, W.G., Blanchere, F.M., Beezhold, D.H., Law, B.F., Derk, R.C., Hettick, J.M., Woodfork, K., Goldsmith, W.T., Harris, J.R., Duling, M.G., Boutin, B., Nurkiewicz, T., Noti, J.D. (2021b). A comparison of performance metrics for cloth masks as source control devices for simulated cough and exhalation aerosols. Aerosol Sci. Technol. 55, 1125–1142. https://doi.org/10.1080/02786826.2021.1933377

Morawska, L., Milton, D.K. (2020). It is time to address airborne transmission of COVID-19. Clin. Infect. Dis. 71, 2311–2313. https://doi.org/10.1093/cid/ciaa939

Parlin, A.F., Stratton, S.M., Culley, T.M., Guerra, P.A. (2020). A laboratory-based study examining the properties of silk fabric to evaluate its potential as a protective barrier for personal protective equipment and as a functional material for face coverings during the COVID-19 pandemic. PLoS One 15, e0239531. https://doi.org/10.1371/journal.pone.0239531

R Core Team (2019). R: A language and environment for statistical computing. https://www.R-project.org/ (accessed 3 April 2022).

Rathinamoorthy, R., Balasaraswathi, S.R. (2021). Disposable tri-layer masks and microfiber pollution – An experimental analysis on dry and wet state emission. Sci. Total Environ. 816, 151562. https://doi.org/10.1016/j.scitotenv.2021.151562

Reutman, S.R., Reponen, T., Yermakov, M., Grinshpun, S.A. (2021). Homemade facemasks: Particle filtration, breathability, fit, and other performance characteristics. J. Occup. Environ. Hyg. 18, 334–344. https://doi.org/10.1080/15459624.2021.1925124

Russell, L. (2018). emmeans: Estimated marginal means, aka Least-Squares Means. R package version 1.3.0. https://github.com/rvlenth/emmeans (accessed 4 April 2022).

Sankhyan, S., Heinselman, K.N., Ciesielski, P.N., Barnes, T., Himmel, M.E., Teed, H., Patel, S.,
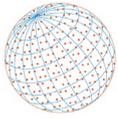
Vance, M.E. (2021). Filtration performance of layering masks and face coverings and the reusability of cotton masks after repeated washing and drying. Aerosol Air Qual. Res. 21, 210117. https://doi.org/10.4209/aaqr.210117

Selvaranjan, K., Navaratnam, S., Rajeev, P., Ravintherakumaran, N. (2021). Environmental challenges induced by extensive use of face masks during COVID-19: A review and potential solutions. Environ. Challenges 3, 100039. https://doi.org/10.1016/j.envc.2021.100039

Sickbert-Bennett, E.E., Samet, J.M., Prince, S.E., Chen, H., Zeman, K.L., Tong, H., Bennett, W.D. (2021). Fitted filtration efficiency of double masking during the COVID-19 pandemic. JAMA Intern. Med. 181, 1126–1127. https://doi.org/10.1001/jamainternmed.2021.2033

Singh, C.P., Vaishna, R.L., Kakkar, A., Arunkumar, K.P., Nagaraju, J. (2014). Characterization of antiviral and antibacterial activity of *Bombyx mori* seroin proteins. Cell. Microbiol. 16, 1354–1365. https://doi.org/10.1111/cmi.12294

Sotirchos, E.S., Fitzgerald, K.C., Crainiceanu, C.M. (2019). Reporting of R^2 statistics for mixed-effects regression models. JAMA Neurol. 76, 507. https://doi.org/10.1001/jamaneurol.2018.4720

The jamovi project (2021). jamovi (Version 1.6). https://www.jamovi.org (accessed 3 April 2022).

Yang, S., Lee, G.W.M., Chen, C.M., Wu, C.C., Yu, K.P. (2007). The size and concentration of droplets generated by coughing in human subjects. J. Aerosol Med. 20, 484–494. https://doi.org/10.1089/jam.2007.0610

Zayas, G., Chiang, M.C., Wong, E., MacDonald, Lange, C.F., Senthilselvan, A., King, M. (2012). Cough aerosol in healthy participants: Fundamental knowledge to optimize droplet-spread infectious respiratory disease management. BMC Pulm. Med. 12, 1–11 https://doi.org/10.1186/1471-2466-12-11

Zhang, Y. (2002). Applications of natural silk protein sericin in biomaterials. Biotechnol. Adv. 20, 91–100. https://doi.org/10.1016/S0734-9750(02)00003-4

Zhang, Y., Tang, M., Dong, Z., Zhao, D., An, L., Zhu, H., Xia, Q., Zhao, P. (2020). Synthesis, secretion, and antifungal mechanism of a phosphatidylethanolamine-binding protein from the silk gland of the silkworm *Bombyx mori*. Int. J. Biol. Macromol. 149, 1000–1007. https://doi.org/10.1016/j.ijbiomac.2020.01.310

Zhu, H., Zhang, X., Lu, M., Chen, H., Chen, S., Han, J., Zhang, Y., Zhao, P., Dong, Z. (2020). Antibacterial mechanism of silkworm seroins. Polymers 12, 2985. https://doi.org/10.3390/polym12122985